



Light-induced structural changes of the LOV2 domains in various phototropins revealed by FTIR spectroscopy

Tatsuya Iwata^{1,2}, Satoru Tokutomi³ and Hideki Kandori²

¹Center for Fostering Young and Innovative Researchers, Nagoya Institute of Technology, Showa-ku, Nagoya 466-8555, Japan

²Department of Frontier Materials, Nagoya Institute of Technology, Showa-ku, Nagoya 466-8555, Japan

³Graduate School of Science, Osaka Prefecture University, Sakai, Osaka 599-8531, Japan

Received July 13, 2011; accepted September 8, 2011

Phototropin (Phot), a blue-light photoreceptor in plants, consists of two FMN-binding domains (named LOV1 and LOV2) and a serine/threonine (Ser/Thr) kinase domain. We have investigated light-induced structural changes of LOV domains, which lead to the activation of the kinase domain, by means of light-induced difference FTIR spectroscopy. FTIR spectroscopy revealed that the reactive cysteine is protonated in both unphotolyzed and triplet-excited states, which is difficult to detect by other methods such as X-ray crystallography. In this review, we describe the light-induced structural changes of hydrogen-bonding environment of FMN chromophore and protein backbone in *Adiantum neo1*-LOV2 in the C=O stretching region by use of ¹³C-labeled samples. We also describe the comprehensive FTIR analysis of LOV2 domains among *Arabidopsis phot1*, *phot2*, and *Adiantum neo1* with and without J α helix domain.

Key words: phototropin, blue-light photoreceptor, LOV domain, FMN, FTIR spectroscopy

Plants have developed many sensory systems to adapt to environmental variations in light, gravity, temperature, and chemical substrates. Light is one of the most important environmental factors for plants because they use it as an

energy source. Plants have three major photoreceptor proteins to sense the intensity, direction, and quality of the light environment. Phytochrome¹ senses red/far-red light and acts as a photoreversible molecular switch. Other photoreceptor proteins, such as cryptochrome² and phototropin^{3–6}, respond to blue light; however, a new class of blue light receptors, FKF1 (flavin-binding Kelch repeat F-box 1) family members (including FKF1⁷, ZTL⁸ and LKP2⁹) respond to UV-A/blue light (320–500 nm). Phototropin (phot), which was originally identified as a photoreceptor for phototropism in *Arabidopsis*¹⁰, has also been found to regulate chloroplast relocation movements^{11–13}, light-induced stomatal opening¹⁴, cotyledon expansion¹⁵, leaf expansion¹⁶, and rapid inhibition of hypocotyl elongation¹⁷. These functions are deeply involved in optimizing the efficiency of photosynthesis. Most higher plants have two isoforms of phot: *phot1* and *phot2*⁶. Stomatal opening is mediated redundantly by both *phot1* and *phot2*¹⁴. In contrast, *phot1* and *phot2* share tropic responses and chloroplast accumulation, depending on the fluence rate of light in *Arabidopsis*¹², whereas chloroplast avoidance is regulated by only *phot2*¹¹. Thus, they share these responses via their different sensitivities to light. In addition to *phot1* and *phot2*, ferns and green algae have a fusion protein of phot in its C-terminus with a chromophoric domain of phytochrome in its N-terminus, which is named neochrome (neo, renamed from phytochrome 3)^{18,19} and acts as a red light sensor. Neo1 from *Adiantum* can also act as a blue light sensor²⁰, although *neo1* and *neo2* from *Mougeotia scalaris* cannot¹⁹.

Phototropin consists of about 1000 amino acid residues and two prosthetic FMN molecules. The FMN-binding

Corresponding author: Hideki Kandori, Department of Frontier Materials, Nagoya Institute of Technology, Gokiso-cho, Showa-ku, Nagoya, Aichi 466-8555, Japan.
e-mail: kandori@nitech.ac.jp

domains are located at the N-terminal half, and the C-terminal half has a serine/threonine (Ser/Thr) kinase domain. The photochemical reaction of FMN yields kinase activation through a change in the domain-domain interaction, although the mechanism is not yet clear. The two FMN-binding domains (ca. 100 residues) are named LOV1 and LOV2, since they have primary²¹ and tertiary²² structures highly homologous to bacterial light-sensor PYP (photoactive yellow protein), oxygen-sensor FixL, and voltage-sensor HERG of a channel protein so that the domain is called the LOV (light, oxygen, and voltage sensing) domain (Fig. 1a). The protein fold belongs to the PAS (Per-Arnt-Sim) superfamily. X-ray crystallography showed that the structures of various LOV domains, LOV1 domains from *Chlamydomonas* phot²³ and *Arabidopsis* phot1 and phot2²⁴ and LOV2 domains from *Adiantum* neo1^{22,25} and oat phot1²⁶, all reported similar protein architectures.

The primary photoreaction in the LOV domain is an adduct formation between FMN and a nearby cysteine^{27–31} (Fig. 1b). After light absorption by FMN, intersystem crossing leads to the formation of a triplet-excited state that absorbs at 660 nm (L660) and appears with a time constant of 3 ns in *Adiantum* neo1-LOV2 and oat phot1-LOV2³². Then, adduct formation accompanies the appearance of the S390 intermediate with time constants of 4 μ s in oat phot1-LOV2²⁹ and 0.9 and 4 μ s in *Chlamydomonas* phot-LOV1³³. Although various models have been proposed for the reactive cysteine, previous FTIR studies revealed that cysteine is protonated in both the ground^{34–38} and triplet-excited³⁹ states of FMN. A dynamical protein motion probably plays an important role in adduct formation⁴⁰.

S390 is the only ground-state intermediate during the photocycle of LOV domains. Therefore, it is believed that S390 is the active state for the light-sensing function of phototropin. Although the crystal structures of the unphotolyzed²² and S390³¹ states of neo1-LOV2 show identical surfaces, our FTIR studies indicate a highly temperature-dependent nature of the amide-I vibrations of neo1-LOV2. Structural perturbation of the loop region is prominent at low temperatures (<250 K), whereas those of the α -helix and β -sheet appear at higher temperatures (>250 K), suggesting the presence of progressive protein structural changes⁴¹. Other FTIR⁴² and circular dichroism (CD) studies⁴³ have also demonstrated that photoactivation of purified LOV2 includes structural changes in the LOV-domain apoprotein. NMR and X-ray crystallographic studies of extended LOV2 fragments from oat phot1 revealed that an extra α -helix (named the $J\alpha$ helix) associates with the surface of LOV2 in the dark state^{26,44,45} (Fig. 1a). The $J\alpha$ helix is located at the C-terminus of LOV2 and is amphipathic in nature, consisting of polar and apolar sides, the latter of which docks onto the β -sheet strands of the LOV2 core. The interaction between $J\alpha$ and LOV2 is disrupted upon cysteinyl adduct formation. Recently, light-induced conformational changes of $J\alpha$ helix were also observed by means of a transient grating

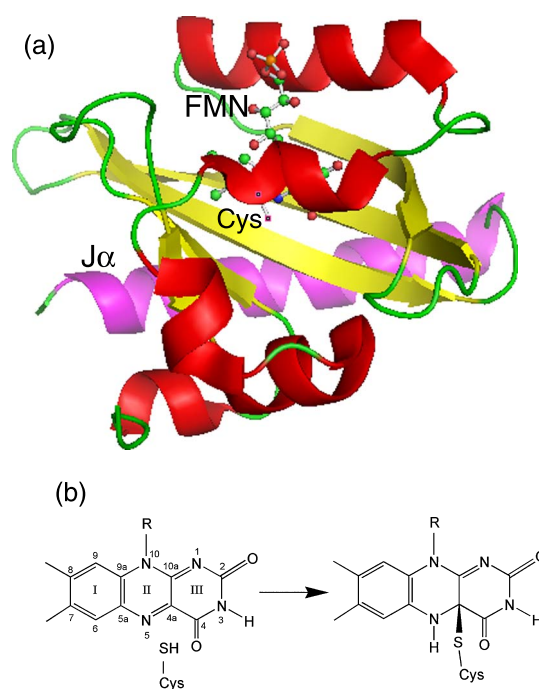


Figure 1 (a) Protein structure of oat phot1-LOV2 (pdb entry 2V1A)²⁶. The whole structure is shown as a ribbon drawing. The helices, turns, and sheets in the LOV-core domain are colored red, green, and yellow, respectively. $J\alpha$ helix is colored magenta. The FMN and reactive cysteine (Cys450 in the oat phot1-LOV2) are shown as a ball-and-stick drawing. The folding motif of this protein is characteristic of the PAS superfamily. Figure was drawn with PyMOL software⁵⁹. (b) Photo-reaction scheme for the LOV domains.

method^{46–49}. However, it is still unclear how the conformational changes in the LOV2 core by the adduct formation are transmitted to the $J\alpha$ helix. Moreover, we have to be careful to accept the scheme as a common mechanism in phototropin because it was made from limited data based on species (neo1, phot1, phot2, etc.) and methods (FTIR, NMR, transient grating, etc.). An important question arises whether protein structural changes in activation of LOV2 domains are common or unique.

We have investigated light-induced structural changes of LOV domains by means of FTIR spectroscopy^{34,37–41,50–53}. In this review, we describe the light-induced structural changes of hydrogen-bonding environment of FMN chromophore and protein backbone in *Adiantum* neo1-LOV2 in the C=O stretching region by use of ¹³C-labeled samples⁵¹. We also describe the comprehensive FTIR analysis of LOV2 domains among *Arabidopsis* phot1, phot2, and *Adiantum* neo1 with and without $J\alpha$ helix domain^{52,53} (Fig. 2).

C=O Stretching Vibrations in *Adiantum* neo1-LOV2 Reconstitution of the FMN Chromophore into the neo1-LOV2 Apoprotein

C=O stretching region of FTIR spectra (amide-I vibrational region of the peptide backbone) is sensitive for

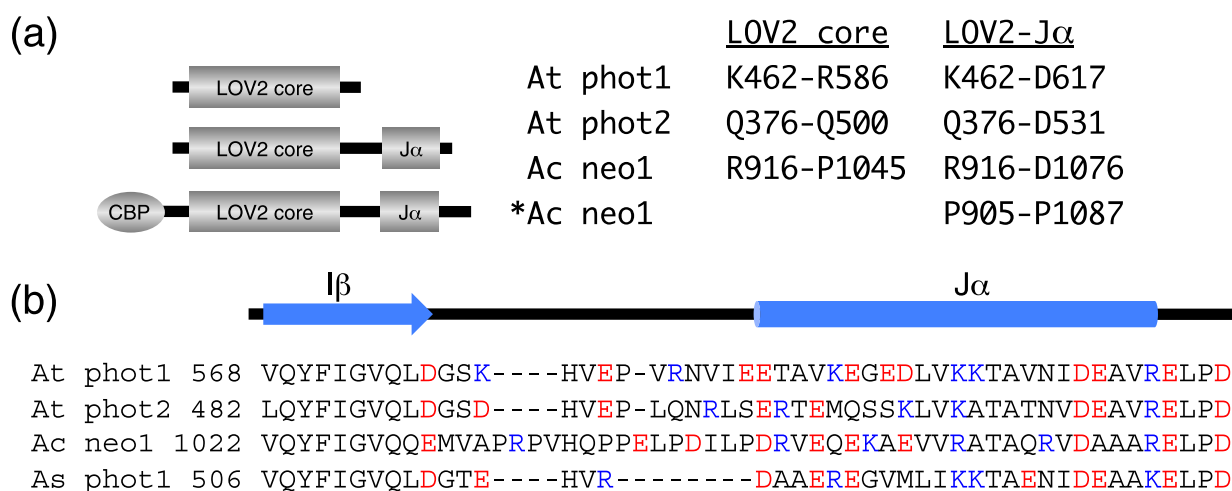


Figure 2 (a) Schematic illustration of the LOV2 constructs of phototropin presented in this review. For the reconstitution of *Adiantum* neo1-LOV2 (*Ac neo1), we used the P905–P1087 construct containing the CBP tag at the N-terminus. For the comparison of the effect of Jα helix, we used the constructs encoding the same region of the LOV2-core and LOV2-Jα for *Arabidopsis* (At) phot1 and phot2 and *Adiantum* (Ac) neo1, where the GST tag at the N-terminus is digested with thrombin. (b) Amino acid sequences of the C-terminal side of LOV2-core and LOV2-Jα. This figure is modified from Ref 53.

secondary structures of peptide backbone of proteins. We previously observed temperature-dependent FTIR spectral changes in the amide-I region for *Adiantum* neo1-LOV2 upon the light illumination⁴¹. Because the frequency region of amide-I vibrations also contains the C=O stretches of FMN, we aimed at assigning C=O stretching vibrations of the FMN and protein by using ¹³C-labeling. The C4=O and C2=O stretching vibrations of FMN and apoprotein were assigned by using [4,10a-¹³C₂] and [2-¹³C] FMNs^{54,55}, and ¹³C-labeled apoprotein, respectively.

We first examined whether the FMN chromophore is properly reconstituted into the original binding site. Figure 3a compares difference FTIR spectra of the S390 and unphotolyzed states between the native (dotted lines) and reconstituted (solid lines) neo1-LOV2 measured at 295 K. The reconstituted neo1-LOV2 sample was prepared by mixing the unlabeled FMN and apoprotein as described in elsewhere⁵¹. Both spectra coincide very well with each other although the spectral deviation was observed. Figure 3a provides criteria of experimental accuracy in the following measurements.

¹³C Isotope Effect of FMN for the Vibrations at 1800–1600 cm⁻¹

C=O stretching vibrations of the FMN and peptide backbone (amide-I) appear at 1800–1600 cm⁻¹. Figure 3b and c shows FTIR difference spectra of neo1-LOV2 reconstituted with unlabeled FMN (solid lines), [4,10a-¹³C₂]FMN (dotted line in b) and [2-¹³C]FMN (dotted line in c) in the 1750–1600 cm⁻¹ region at 295 K, respectively. The bands at 1730–1710 cm⁻¹ are attributable to the C4=O stretching vibration because a clear isotope effect was observed for [4,10a-¹³C₂]FMN (Fig. 3b) but not for [2-¹³C]FMN (Fig. 3c). The

bands at 1730 (+)/1711 (–) cm⁻¹ (Fig. 3b) were not observed by ¹³C labeling of the C4=O group, probably because they downshifted. The remaining bands (~15%) may originate from incomplete reconstitution of FMN. For substitution of ¹²C to ¹³C, the spectral downshift is expected to be 35–40 cm⁻¹, calculated from the square root of reduced mass ratio between ¹²C=O and ¹³C=O. Because strong bands of amide-I vibrations mask such shifted bands, we examined the detailed isotope shift by calculating double difference spectra. Figure 3d shows the double difference spectrum, where the labeled spectrum (dotted line in Fig. 3b) was subtracted from the unlabeled one (solid line in Fig. 3b). Such spectral analysis indicates that the bands at 1730 (+) and 1711 (–) cm⁻¹ exhibit downshifts to 1676 and 1661 cm⁻¹ by ¹³C4 labeling, respectively. A larger spectral downshift (about 50 cm⁻¹) was also observed for FMN in solution and explained in terms of vibrational coupling of the C4=O stretch and the N3-H bend for the FMN in solution⁵⁵.

Figure 3c shows significant isotope effects at 1700–1650 cm⁻¹ for the ¹³C-labeling at the C2 position. Corresponding double difference spectra are shown in Figure 3e. As clearly shown in Figure 3e, the C2=O stretching vibrations of the unphotolyzed and S390 states can be assigned to the 1677 and 1686 cm⁻¹ bands, which shift to 1641 and 1654 cm⁻¹, respectively. Isotope shifts are smaller than those for the C4=O stretch, which may suggest that the C2=O stretch is an isolated mode.

Both C4=O and C2=O stretching vibrations shift to higher frequencies upon the formation of S390 (Fig. 3), which was essentially temperature-independent⁵¹. This shows that the hydrogen bonds of the C=O groups are weakened by adduct formation, which presumably relocates the FMN chromophore apart from their hydrogen-bonding donors.

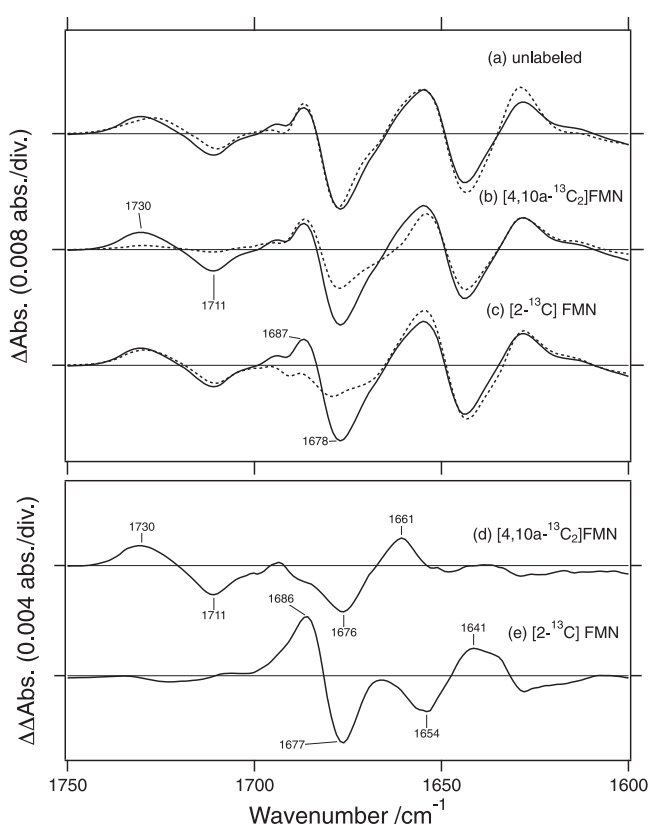


Figure 3 (a) Difference FTIR spectra of native neo1-LOV2 (dotted lines) and neo-LOV2 reconstituted with the FMN and apoprotein (solid lines) in the 1800–950 cm^{-1} region at 295 K. (b and c) Difference FTIR spectra of neo1-LOV2 reconstituted with unlabeled FMN (solid lines), [4,10a- $^{13}\text{C}_2$]FMN (dotted line in b) and [2- ^{13}C]FMN (dotted line in c). (d and e) Double-difference spectra of those in Figure 3b and c, where the labeled spectra (dotted lines) are subtracted from the unlabeled spectra (solid lines). This figure is modified from Ref 51.

The conformational switch of Gln1029 may also contribute to the frequency change in S390⁵⁰. It should be noted, however, that there is a certain temperature-dependence for the C4=O and C2=O stretching vibrations in the S390 state but in the unphotolyzed state. The frequencies of the C4=O stretch in S390 are 1723 and 1730 cm^{-1} at 150 and 295 K, respectively, whereas those of the C2=O stretch in S390 are 1687 and 1683 cm^{-1} at 150 and 295 K, respectively (see below; Fig. 4). These frequency shifts possibly originate from temperature-dependent chromophore-protein interaction changes.

^{13}C Isotope Effect of Protein for the Vibrations at 1800–1600 cm^{-1}

We then introduced ^{13}C -labeling into the protein of neo1-LOV2. Figure 4a compares the difference FTIR spectra of neo1-LOV2 reconstituted with unlabeled FMN at 150 K, where apoprotein is ^{13}C -labeled (lower trace) and unlabeled (upper trace). In the amide-I region, isotope effect was seen; the bands of the unlabeled protein at 1692 (+), 1660 (+), and 1646 (–) cm^{-1} disappeared (upper trace), whereas the bands

at 1647 (+), 1639 (–), 1618 (+), and 1605 (–) cm^{-1} newly appeared for the ^{13}C -labeling of protein (bottom trace) at 150 K. The signal intensity at 1673 (–) cm^{-1} was reduced upon ^{13}C -labeling of the protein. The spectral feature is remarkably different at 295 K, where $^{13}\text{C}=\text{O}$ bands appeared at 1614 (+), 1603 (–), and 1588 (+) cm^{-1} (lower trace in Fig. 4b) more strongly than those at 150 K.

In Figure 4a, the bands at 1723 (+), 1710 (–), and 1688 (+) cm^{-1} were not shifted for ^{13}C -labeling of the protein. On the other hand, the bands at 1692 (+), 1673 (–), 1660 (+), and 1646 (–) cm^{-1} exhibited an isotope effect, presumably shifting to 1647 (+), 1639 (–), 1618 (+), and 1605 (–) cm^{-1} , respectively. The band at 1673 (–) cm^{-1} was split into two bands for ^{13}C -labeling of protein, the remaining band at 1675 cm^{-1} and the shifted band at 1639 cm^{-1} . Thus, the red spectrum in Figure 4a clearly demonstrates the successful separation of the bands at 1750–1650 cm^{-1} into those of the FMN and protein. As we showed in Figure 3, the bands at 1723 (+)/1710 (–) and 1687 (+)/1675 (–) (1688 (+)/1673 (–)) cm^{-1} originate from the C4=O and C2=O stretching vibrations of FMN, respectively. On the other hand, the bands at 1692 (+)/1673 (–) and 1660 (+)/1646 (–) cm^{-1} , which shift to 1647 (+)/1639 (–) and 1618 (+)/1605 (–) cm^{-1} , respectively, come from amide-I vibrations. From the frequencies, the bands at 1673 and 1646 cm^{-1} in the unphotolyzed state correspond to the loop structure and α -helix, respectively. We previously inferred the protein structural change in the loop and α -helix regions at 150 K⁴¹, which is now experimentally unambiguous.

In Figure 4b, the bands at 1730 (+), 1711 (–), and 1687 (+) cm^{-1} were not shifted for ^{13}C -labeling of the protein, which originate from C=O stretching vibrations of FMN. It should be noted that the bands at 1644 (–) and 1629 (+) cm^{-1} apparently look unshifted, suggesting that they are also attributable to the vibrations of FMN such as ring I vibration^{35,42}. However, if this is the case, the bands must appear in the spectrum at 150 K because the structural changes of the FMN are similar between 150 and 295 K (Fig. 3). No corresponding bands at 150 K (Fig. 4a) imply that the bands at 1644 (–) and 1629 (+) cm^{-1} originate from the protein, not from vibrations of FMN.

The bands at 1655 (+), 1644 (–), and 1629 (+) cm^{-1} exhibited isotope effects, presumably shifting to 1614 (+), 1603 (–), and 1588 (+) cm^{-1} , respectively. Similar to that at 150 K, the band at 1678 (–) cm^{-1} was probably split into two bands for ^{13}C -labeling of protein: the remaining band at 1673 (–) cm^{-1} and the shifted band at 1642 (–) cm^{-1} . Interestingly, the red spectrum shows an additional positive band at 1630 cm^{-1} . The band appears to originate from protein, because the bands at 1644 (–)/1629 (+) cm^{-1} are insensitive to ^{13}C -labeling of FMN (Fig. 3). Thus, it is likely that the band at 1655 (+) cm^{-1} was probably split into two bands by the isotope shift, 1630 and 1614 cm^{-1} (Fig. 4b). The origins of the bands at 1730 (+)/1711 (–) and 1687 (+)/1678 (–) cm^{-1} are the C4=O and C2=O stretching vibrations of FMN,

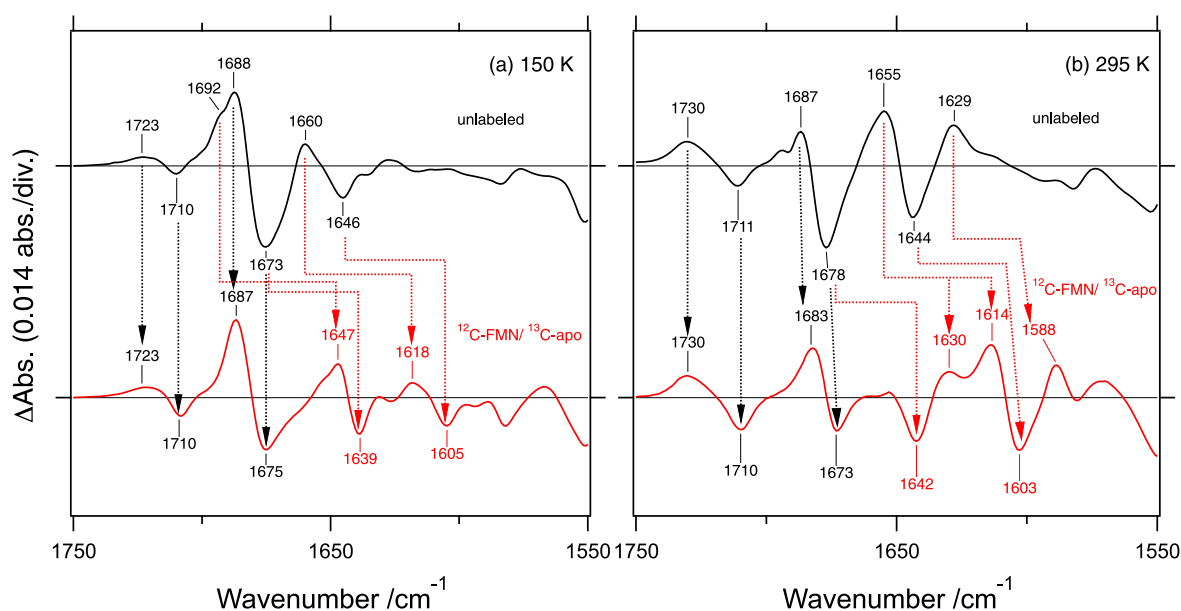


Figure 4 Difference FTIR spectra of unlabeled neo1-LOV2 (upper traces) and ^{12}C -FMN/ ^{13}C -apoprotein neo1-LOV2 (lower traces) in the 1750–1550 cm^{-1} region at 150 K (a) and 295 K (b). The corresponding signals are connected by dotted arrows. This figure is modified from Ref 51.

respectively. On the other hand, the bands at 1678 (–)/1655 (+) and 1644 (–)/1629 (+) cm^{-1} originate from amide-I vibrations.

As at 150 K, the successful separation of the bands into those of FMN and protein by using ^{13}C -labeling of protein is advantageous in analyzing protein structural changes at 295 K. There are five peaks for the $^{13}\text{C}=\text{O}$ stretching vibrations at 1642 (–), 1630 (+), 1614 (+), 1603 (–), and 1588 (+) cm^{-1} (red line in Fig. 4b). Negative bands at 1642 and 1603 cm^{-1} also appeared at 150 K. Thus, amide-I bands can be assigned as follows. The bands at 1642 (–)/1630 (+) cm^{-1} originate from the amide-I vibration of the loop region, whereas those at 1614 (+)/1603 (–) cm^{-1} come from the amide-I vibration of the α -helix. The additional positive peak at 1588 cm^{-1} at 295 K, not at 150 K, can be assigned to the amide-I vibration of the β -sheet. The corresponding negative band is probably located at 1603 (–) cm^{-1} .

During the photocycle of LOV domains, S390 is the only ground-state intermediate^{29,32,33}. Therefore, it is believed that S390 is the active state for the light-sensing function of phototropin. However, our FTIR study showed a highly temperature-dependent nature for amide-I vibrations of neo1-LOV2⁴¹, suggesting that progressive protein structural changes take place in the S390 state. This conclusion was deduced from the spectral analysis of amide-I vibrations at 1700–1600 cm^{-1} .

The hydrogen bond of the peptide backbone in the loop region (1673 cm^{-1}) is weakened at low temperatures (1692 cm^{-1}) but is strengthened at room temperature (1655 cm^{-1}). On the other hand, helical structural perturbation was rather temperature independent, exhibiting a weakened hydrogen bond upon S390 formation (1644 to 1655 cm^{-1}). The reac-

tive cysteine (Cys966 for neo1-LOV2) is located at the joint between helical and connected turn structures (Fig. 1a).

The difference FTIR spectra at 150 K probably include the structural changes in this region. Interestingly, the red spectrum in Figure 4a shows that all bands in the 1750–1600 cm^{-1} region shift to higher frequencies upon the formation of S390, such as 1710 to 1723 cm^{-1} , 1675 to 1687 cm^{-1} , 1639 to 1647 cm^{-1} , and 1605 to 1618 cm^{-1} . This indicates weakened hydrogen bonds of the C4=O and C2=O groups of the FMN and the C=O groups of the peptide backbone. It seems that the formation of a new covalent bond between the chromophore and protein in S390 weakens other chromophore-protein interactions and protein structure, which was observed at 150 K.

At higher temperatures such as 295 K, the secondary structure of the protein is altered from that at 150 K. The hydrogen bond of the loop structure is now strengthened at room temperature, whereas structural changes of the α -helix are similar between those at 150 and 295 K. In addition, the structural perturbation of the β -sheet is newly observed only at room temperature. These changes probably correspond to the local-to-global protein structural alterations, and the structure of S390 at 295 K represents the signaling state. It should be noted that the loop structures changing at 150 and 295 K are not necessarily identical in position because hydrogen bonding strength of the loop region in the S390 intermediate are weakened at 150 K (upshift from 1675 to 1687 cm^{-1}) but strengthened at 295 K (downshift from 1678 to 1655 cm^{-1}). We previously identified O-H stretches of the internal water molecules of neo1-LOV2, and the water bands were temperature independent⁵⁸. These water molecules are bound near Cys966 in the loop region. This may suggest

that the loop structure observed at 295 K originates from a different part observed at 150 K.

Structural Changes of the LOV2 Domain and the J α Helix among Phototropins

Light-Induced Difference FTIR Spectra of LOV2-core and LOV2-J α in *Arabidopsis* Phot1

At the C-terminal side of the LOV2 domain, there is an α -helix called the J α helix (Fig. 1a). The functional importance of the J α helix has been established for *Arabidopsis* phot1, where light-induced structural perturbation takes place in the J α helix during the photocycle of LOV2 domains⁴⁵. However, the FTIR study reports a different role of the J α helix in light-induced signal transduction of LOV2 domains. We constructed LOV2 domains with (LOV-J α) and without (LOV-core) the J α helix for *Arabidopsis* phot1 and phot2 and *Adiantum* neo1 and compare their light-induced difference FTIR spectra.

Figure 5 shows light-induced difference FTIR spectra of LOV2-core (dotted lines) and LOV2-J α (solid lines) for *Arabidopsis* phot1 (a), *Arabidopsis* phot2 (b), and *Adiantum* neo1 (c) in the 1750–1600 cm^{-1} region. The light-induced difference spectra were measured in a wide temperature range (150–295 K). In addition to the amide-I vibrations, the C2=O and C4=O stretching vibrations of FMN also appear in this frequency region. Our study of neo1-LOV2 identified the frequencies at 1677 and 1711 cm^{-1} as the C2=O and C4=O stretching vibrations by use of ¹³C2=O- and ¹³C4=O-labeled FMN (Fig. 3). Similarly, negative bands at 1676 and

1712 cm^{-1} in Figure 5a and at 1678 and 1713 cm^{-1} in Figure 5b presumably originate from these vibrations in the unphotolyzed states of phot1 and phot2. It is likely that a higher frequency shift of both C2=O and C4=O stretches occurs in Figure 5, implying common structural changes of FMN among phot1, phot2, and neo1. Similar changes between LOV2-core and LOV2-J α also indicate that the presence of the J α helix does not affect structural perturbation of FMN.

All other vibrations in this frequency region originate from those from protein, particularly amide-I modes reflecting C=O stretches of the peptide backbone. It is well-known that the amide-I frequencies are characteristic of secondary structures, such as a loop (1670–1690 cm^{-1}), an α -helix (\sim 1650 cm^{-1}), and a β -sheet (1620–1640 cm^{-1}). Figure 5a shows prominent spectral alterations at 1650–1600 cm^{-1} between LOV2-core and LOV2-J α . At 150 and 250 K, there are no significant differences at this frequency (Fig. 5a), implying structural changes of neither the α -helix nor the β -sheet. On the other hand, prominent peaks newly appeared at 1650 (–) and 1625 (+) cm^{-1} at 260, 273, and 295 K for LOV2-J α (solid lines). The negative 1650 cm^{-1} band, characteristic for the α -helix, was not observed for LOV2-core, and we interpreted that disruption of the α -helix structure presumably originates from the J α helix⁵². This interpretation was further supported by the fact that such spectral changes were diminished by point mutation of functionally important amino acids such as Phe556 between FMN and the β -sheet, Gln575 being hydrogen-bonded with FMN, and Ile608 on the J α helix (Figs. 1 and 2)⁵².

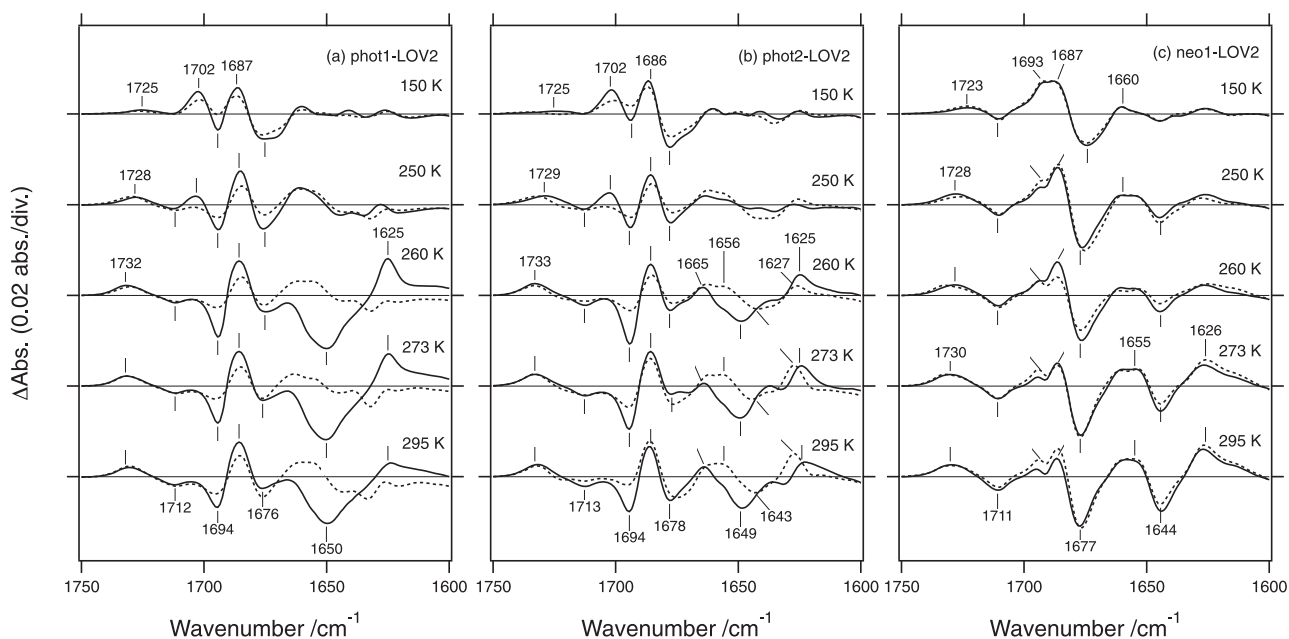


Figure 5 Light-induced difference FTIR spectra for the LOV2 domain of *Arabidopsis* phot1(a), *Arabidopsis* phot2 (b), and *Adiantum* neo1 (c) in the 1750–1600 cm^{-1} region. LOV2-core (dotted lines) and LOV2-J α (solid lines) are shown. The spectra were recorded at 150, 250, 260, 273, and 295 K. This figure is modified from Ref 52 and 53.

Light-Induced Difference FTIR Spectra of LOV2-core and LOV2-J α in *Arabidopsis* Phot2

Essentially similar spectral features were observed for *Arabidopsis* phot2-LOV2 (Fig. 5b). At 150 and 250 K, solid and dotted spectra are similar, particularly in the amide-I region, indicating that the structural changes in phot2-LOV2 are not affected by the existence of the J α helix. In particular, little spectral difference at 1650–1600 cm⁻¹ is the same as in phot1-LOV2 (Fig. 5a), indicating little effect of J α at 150 and 250 K. In contrast, a clear spectral difference was observed between LOV2-core and LOV2-J α at 260 K. A negative peak at 1649 cm⁻¹ only appears in LOV2-J α , but not in LOV2-core. The corresponding positive peak is presumably at 1625 cm⁻¹, and these spectral features are similar between phot1 (Fig. 5a) and phot2 (Fig. 5b).

Although the appearance of a peak pair at 1649 (-)/1625 (+) cm⁻¹ in LOV2-J α is common, an obvious difference was also seen between *Arabidopsis* phot1 and phot2. The most noticeable observation in phot2 was a positive peak at 1627 cm⁻¹ for LOV2-core. This peak is close in frequency to that at 1625 cm⁻¹ in LOV2-J α , and the intensity in LOV2-core is smaller at 260 K, equal at 273 K, and larger at 295 K than that in LOV2-J α (Fig. 5b). Such a spectral feature was never observed for phot1 (Fig. 5a). The corresponding negative band of the band at 1627 (+) cm⁻¹ must be located at 1643 cm⁻¹, and there is an additional positive peak at 1656 cm⁻¹ (Fig. 5b). It should be noted that the bands at 1656 (+)/1643 (-)/1627 (+) cm⁻¹ for phot2 LOV2-core were observed in neo1-LOV2 (Fig. 5c; see below)^{41,51}. Thus, it is likely that in phot2-LOV2 structural changes in the α -helix and β -sheet regions take place without the J α helix.

Influence of the J α helix can be seen for the negative band at 1694 cm⁻¹ for both phot1 (Fig. 5a) and phot2 (Fig. 5b). In both cases, the negative 1694 cm⁻¹ band intensified in the presence of the J α helix. This is also the case at 150 and 250 K, which can be seen more clearly in the double difference spectra (see below; Fig. 6). Since the C2=O and C4=O stretching vibrations of FMN are located at 1676–1678 and 1712–1713 cm⁻¹, respectively, the negative band probably originates from an amide-I vibration that corresponds to the loop structure. The corresponding positive band is presumably located at 1686–1687 cm⁻¹, where a lower frequency indicates the strengthened hydrogen bond of the loop structure.

Light-Induced Difference FTIR Spectra of LOV2-core and LOV2-J α in *Adiantum* neo1

Entirely different spectral features on the influence of the J α helix were obtained for *Adiantum* neo1-LOV2. Figure 5c shows almost identical differences in FTIR spectra between LOV2-core (dotted lines) and LOV2-J α (solid lines) at any temperature. This indicates neither structural changes of the J α helix itself nor J α -dependent structural changes of other parts upon photoactivation of neo1-LOV2. By using ¹³C labeling, we identified the bands at 1730–1723 (+)/1711 (-)

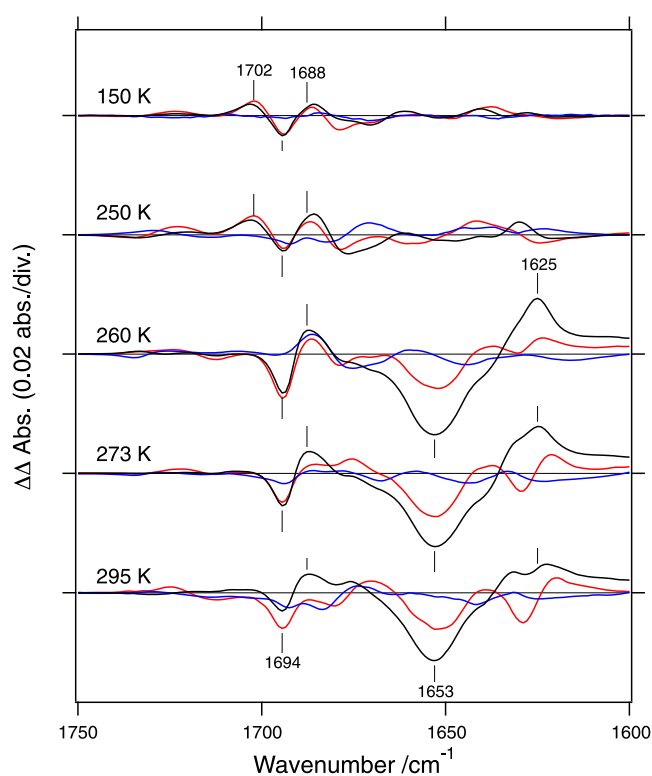


Figure 6 Double difference spectra between the LOV2-J α and LOV2 core in the 1750–1600 cm⁻¹ region. Spectra of phot1 (black lines), phot2 (red lines), and neo1 (blue lines) are shown at 150, 250, 260, 273, and 295 K. This figure is modified from Ref 53.

/1687 (+)/1677 (-) cm⁻¹ as C=O stretching vibrations of FMN and the bands at 1693 (+)/1677 (-)/1660 (+)/1655 (+)/1644 (-)/1626 cm⁻¹ as amide-I vibrations (Figs. 3 and 4). As shown in Figure 4, a temperature-dependent nature is obvious; the amide-I band of the loop (1677 cm⁻¹) is shifted up (1693 cm⁻¹) at a low temperature but shifted down (1655 cm⁻¹) at room temperature (Fig. 5c). In addition, the bands at 1644 (-)/1626 (+) cm⁻¹ are intensified as temperature increases, and we previously interpreted the negative 1644 cm⁻¹ band as structural perturbation of the β -sheet⁴¹. It should be noted that the negative peak at 1644 cm⁻¹ could also be assignable as an α -helix only from the frequency, but the band was also observed for LOV2-core, which excludes the possibility of the negative 1644 cm⁻¹ band from the J α helix.

It should also be noted that the construct of neo1-LOV2 for the J α helix study is different from the construct for the assignment of C=O stretching bands (Figs. 3 and 4). We used neo1-LOV2 containing P905-P1087 with a calmodulin binding peptide (CBP) tag for the assignment of C=O stretching bands (Fig. 2a). In contrast, the construct for the J α helix study is slightly shorter (R916-D1076 for LOV2-J α ; Fig. 2a), and no tags are involved. Since such a difference might influence the spectra, we compared the spectra⁵³. We concluded that the J α helix does not affect light-induced

protein structural changes in *Adiantum* neo1-LOV2, which is in high contrast to *Arabidopsis* phot1 and phot2.

Double Difference Spectra of LOV2-core and LOV2-J α

The influence of the J α helix on protein structural changes of LOV2 domains was very different among phot1, phot2, and neo1. Such a difference is obviously seen by subtracting the dotted spectrum from the solid one in Figure 5. Figure 6 shows such double difference spectra of phot1 (black lines), phot2 (red lines), and neo1 (blue lines). It should be noted that each difference spectrum can be quantitatively compared among phot1, phot2, and neo1, because the difference spectra in Figure 3 are normalized by use of vibrational bands at 1500–1200 cm⁻¹⁵². In phot1, the bands at 1653 (-)/1625 (+) cm⁻¹ at 260–295 K originate from the J α -dependent α -helical perturbation (Fig. 6), which is presumably owing to the J α helix itself. There are additional bands in the 1700–1680 cm⁻¹ region: bands at 1702 (+)/1694 (-)/1688 (+) cm⁻¹ at 150 and 250 K and at 1694 (-)/1688 (+) cm⁻¹ at 260–295 K (Fig. 6). It is likely that such a spectral feature at 1700–1680 cm⁻¹ is also seen in phot2 (red lines in Fig. 6). In phot2, the influence of the J α helix is clear (Fig. 5b), but the spectral feature at 1650–1600 cm⁻¹ is more complex than in phot1. Figure 6 shows the presence of a negative band at about 1650 cm⁻¹ in phot2 at 260–295 K, but the amplitude is about half of phot1. In addition, a peak pair was seen at about 1625 cm⁻¹ in Figure 6 (red lines), which originates from two positive peaks at 1627 and 1625 cm⁻¹ in Figure 5b.

Blue lines in Figure 6 were featureless when compared with black and red lines, indicating no effect of the J α helix on protein structural changes of neo1-LOV2. In summary, three phototropins exhibited different effects of the J α helix. In *Arabidopsis* phot1-LOV2, the J α helix is structurally perturbed upon activation as shown by the J α -dependent 1650 (-)/1625 (+) cm⁻¹ bands. In contrast, no changes were gained between LOV2-J α and LOV2-core for *Adiantum* neo1. Interestingly, *Arabidopsis* phot2-LOV2 exhibits an intermediate property between *Arabidopsis* phot1-LOV2 and *Adiantum* neo1-LOV2. Namely, LOV2-core shows 1643 (-)/1627 (+) cm⁻¹ bands (dotted lines in Fig. 5b) that resemble those in neo1-LOV2 (Fig. 5c). In contrast, LOV2-J α shows J α -dependent 1649 (-)/1625 (+) cm⁻¹ bands (solid lines in Fig. 5b) that resemble those in phot1-LOV2 (Fig. 5a). Thus, the observation suggests that the kinase activation mechanisms are different among LOV2 domains.

Conclusion

By means of light-induced difference FTIR spectroscopy and ¹³C-labeling, we have shown structural changes of hydrogen-bonding environment of FMN, protein backbone of LOV-core and J α helix in LOV2 domains of *Arabidopsis* phot1, phot2, and *Adiantum* neo1. Both C4=O and C2=O stretching vibrations shift to higher frequencies upon the formation of S390 for neo1-LOV2, suggesting that the

hydrogen bonds of the C=O groups are weakened by adduct formation.

Light-induced protein structural changes differ significantly between LOV-J α and LOV-core for *Arabidopsis* phot1. In contrast, the difference spectra are identical between LOV-J α and LOV-core for *Adiantum* neo1. In *Arabidopsis* phot2, the protein structural changes are intermediate between *Arabidopsis* phot1 and *Adiantum* neo1. These results suggest that the conformational changes of the J α helix and the interaction between the LOV-core and the J α helix are different among phototropins.

Acknowledgment

We thank A. Yamamoto and T. Koyama for valuable discussion. Some of the researches described here were supported by grants from Japanese Ministry of Education, Culture, Sports, Science, and Technology, and by the Japan Science and Technology Agency to T. I., S. T. and H. K.

REFERENCES

1. Quail, P. H. Photosensory perception and signaling in plant cells: new paradigms? *Curr. Opin. Cell Biol.* **14**, 180–188 (2002).
2. Lin C. & Shalitin, D. Cryptochrome structure and signal transduction. *Annu. Rev. Plant Biol.* **54**, 469–496 (2003).
3. Briggs, W. R. & Christie, J. M. Phototropins 1 and 2: versatile plant blue-light receptors. *Trends Plant Sci.* **7**, 204–210 (2002).
4. Crosson, S., Rajagopal, S. & Moffat, K. The LOV domain family: photoresponsive signaling modules coupled to diverse output domains. *Biochemistry* **42**, 2–10 (2003).
5. Celaya, R. B. & Liscum, E. Phototropins and associated signaling: providing the power of movement in higher plant. *Photochem. Photobiol.* **81**, 73–80 (2005).
6. Briggs, W. R., Beck, C. F., Cashmore, A. R., Christie, J. M., Hughes, J., Jarillo, J. A., Kagawa, T., Kanegae, H., Liscum, E., Nagatani, A., Okada, K., Salomon, M., Rüdiger, W., Sakai, T., Takano, M., Wada, M. & Watson J. C. The phototropin family of photoreceptors. *Plant Cell* **13**, 993–997 (2001).
7. Imaizumi, T., Tran, H. G., Swartz, T. E., Briggs, W. R. & Kay, S. A. FKF1 is essential for photoperiodic-specific light signaling in *Arabidopsis*. *Nature* **426**, 302–306 (2003).
8. Mas, P., Kim, W. Y., Somers, D. E. & Kay, S. A. Targeted degradation of TOC1 by ZTL modulates circadian function in *Arabidopsis thaliana*. *Nature* **426**, 567–570 (2003).
9. Fukamatsu, Y., Mitsui, S., Yasuhara, M., Tokioka, Y., Ihara, N., Fujita, S. & Kiyosue, T. Identification of LOV KELCH PROTEIN2 (LKP2)-interacting factors that can recruit LKP2 to nuclear bodies. *Plant Cell Phys.* **46**, 1340–1349 (2005).
10. Christie, J. M., Reymond, P., Powell, G. K., Bernasconi, P., Reibekas, A. A., Liscum, E. & Briggs, W. R. *Arabidopsis* NPH1: a flavoprotein with the properties of a photoreceptor for phototropism. *Science* **282**, 1698–1701 (1998).
11. Kagawa, T., Sakai, T., Suetsugu, N., Oikawa, K., Ishiguro, S., Kato, T., Tabata, S., Okada, K. & Wada, M. *Arabidopsis* NPL1: a phototropin homolog controlling the chloroplast high-light avoidance response. *Science* **291**, 2138–2141 (2001).
12. Sakai, T., Kagawa, T., Kasahara, M., Swartz, T. E., Christie, J. M., Briggs, W. R., Wada, M. & Okada, K. *Arabidopsis* nph1 and npl1: blue light receptors that mediate both phototropism and chloroplast relocation. *Proc. Natl. Acad. Sci. U.S.A.* **98**,

- 6969–6974 (2001).
13. Jarillo, J. A., Gabrys, H., Capel, J., Alonso, J. M., Ecker, J. R. & Cashmore, A. R. Phototropin-related NPL1 controls chloroplast relocation induced by blue light. *Nature* **410**, 952–954 (2001).
 14. Kinoshita, T., Doi, M., Suetsugu, N., Kagawa, T., Wada, M. & Shimazaki, K. Phot1 and phot2 mediate blue light regulation of stomatal opening. *Nature* **414**, 656–660 (2001).
 15. Ohgishi, M., Saji, K., Okada, K. & Sakai, T. Functional analysis of each blue light receptor, cry1, cry2, phot1, and phot2, by using combinatorial multiple mutants in *Arabidopsis*. *Proc. Natl. Acad. Sci. U.S.A.* **101**, 2223–2228 (2004).
 16. Sakamoto, K. & Briggs, W. R. Cellular and subcellular localization of phototropin 1. *Plant Cell* **14**, 1723–1735 (2002).
 17. Folta, K. M. & Spalding, E. P. Unexpected roles for cryptochrome 2 and phototropin revealed by high-resolution analysis of blue light-mediated hypocotyl growth inhibition. *Plant J.* **26**, 471–478 (2001).
 18. Nozue, K., Kanegae, T., Imaizumi, T., Fukada, S., Okamoto, H., Yeh, K.-C., Lagarias, J. C. & Wada, M. A phytochrome from the fern *Adiantum* with features of the putative photoreceptor NPH1. *Proc. Natl. Acad. Sci. U.S.A.* **95**, 15826–15830 (1998).
 19. Suetsugu, N., Mittmann, F., Wagner, G., Hughes, J. & Wada, M. A chimeric photoreceptor gene, NEOCHROME, has arisen during plant evolution. *Proc. Natl. Acad. Sci. U.S.A.* **102**, 8601–8606 (2005).
 20. Kanegae, T., Hayashida, E., Kuramoto, C. & Wada, M. A single chromoprotein with triple chromophores acts as both a phytochrome and a phototropin. *Proc. Natl. Acad. Sci. U.S.A.* **103**, 17997–18001 (2006).
 21. Huala, E., Oeller, P. W., Liscum, E., Han, I. S., Larsen, E. & Briggs, W. R. *Arabidopsis* NPH1: a protein kinase with a putative redox-sensing domain. *Science* **278**, 2120–2123 (1997).
 22. Crosson, S. & Moffat, K. Structure of a flavin-binding plant photoreceptor domain: insights into light-mediated signal transduction. *Proc. Natl. Acad. Sci. U.S.A.* **98**, 2995–3000 (2001).
 23. Fedorov, R., Schlichting, I., Hartmann, E., Domratcheva, T., Fuhrmann, M. & Hegemann, P. Crystal structures and molecular mechanism of a light-induced signaling switch: the Phot-LOV1 domain from *Chlamydomonas reinhardtii*. *Biophys. J.* **84**, 2474–248 (2003).
 24. Nakasako, M., Zikihara, K., Matsuoka, D., Katsura, H. & Tokutomi, S. Structural basis of the LOV1 dimerization of *Arabidopsis* phototropins 1 and 2. *J. Mol. Biol.* **381**, 718–733 (2008).
 25. Crosson, S. & Moffat, K. Photoexcited structure of a plant photoreceptor domain reveals a light-driven molecular switch. *Plant Cell* **14**, 1067–1075 (2002).
 26. Halavaty, A. S. & Moffat, K. N- and C-terminal flanking regions modulate light-induced signal transduction in the LOV2 domain of the blue light sensor phototropin 1 from *Avena sativa*. *Biochemistry* **46**, 14001–14009 (2007).
 27. Salomon, M., Christie, J. M., Knieb, E., Lempert, U. & Briggs, W. R. Photochemical and mutational analysis of the FMN-binding domains of the plant blue light receptor, phototropin. *Biochemistry* **39**, 9401–9410 (2000).
 28. Miller, S. M., Massey, V., Ballou, D., Williams Jr., C. H., Distefano, M. D., Moore, M. J. & Walsh, C. T. Use of a site-directed triple mutant to trap intermediates: demonstration that the flavin C(4a)-thiol adduct and reduced flavin are kinetically competent intermediates in mercuric ion reductase. *Biochemistry* **29**, 2831–2841 (1990).
 29. Swartz, T. E., Corchnoy, S. B., Christie, J. M., Lewis, J. W., Szundi, I., Briggs, W. R. & Bogomolni, R. A. The photocycle of a flavin-binding domain of the blue light photoreceptor phototropin. *J. Biol. Chem.* **276**, 36493–36500 (2001).
 30. Salomon, M., Eisenreich, W., Dürr, H., Schleicher, E., Knieb, E., Massey, V., Rüdiger, W., Müller, F., Bacher, A. & Richter, G. An optomechanical transducer in the blue light receptor phototropin from *Avena sativa*. *Proc. Natl. Acad. Sci. U.S.A.* **98**, 12357–12361 (2001).
 31. Crosson, S. & Moffat, K. Photoexcited structure of a plant photoreceptor domain reveals a light-driven molecular switch. *Plant Cell* **14**, 1067–1075 (2002).
 32. Kennis, J. T., Crosson, S., Gauden, M., van Stokkum, I. H., Moffat, K. & van Grondelle, R. Primary reactions of the LOV2 domain of phototropin, a plant blue-light photoreceptor. *Biochemistry* **42**, 3385–3392 (2003).
 33. Kottke, T., Heberle, J., Hehn, D., Dick, B. & Hegemann, P. Phot-LOV1: photocycle of a blue-light receptor domain from the green alga *Chlamydomonas reinhardtii*. *Biophys. J.* **84**, 1192–1201 (2003).
 34. Iwata, T., Tokutomi, S. & Kandori, H. Photoreaction of the cysteine S-H group in the LOV2 domain of *Adiantum* phytochrome3. *J. Am. Chem. Soc.* **124**, 11840–11841 (2002).
 35. Ataka, K., Hegemann, P. & Heberle, J. Vibrational spectroscopy of an algal Phot-LOV1 domain probes the molecular changes associated with blue-light reception. *Biophys. J.* **84**, 466–474 (2003).
 36. Bednarz, T., Losi, A., Gartner, W., Hegemann, P. & Heberle, J. Functional variations among LOV domains as revealed by FT-IR difference spectroscopy. *Photochem. Photobiol. Sci.* **3**, 575–579 (2004).
 37. Iwata, T., Nozaki, D., Tokutomi, S. & Kandori, H. Comparative investigation of the LOV1 and LOV2 domains in *Adiantum* phytochrome3. *Biochemistry* **44**, 7427–7434 (2005).
 38. Sato, Y., Nabeno, M., Iwata, T., Tokutomi, S., Sakurai, M. & Kandori, H. Heterogeneous environment of the S-H group of Cys966 near the flavin chromophore in the LOV2 domain of *Adiantum* neochrome1. *Biochemistry* **46**, 10258–10265 (2007).
 39. Sato, Y., Iwata, T., Tokutomi, S. & Kandori, H. Reactive cysteine is protonated in the triplet excited state of the LOV2 domain in *Adiantum* phytochrome3. *J. Am. Chem. Soc.* **127**, 1088–1089 (2005).
 40. Nozaki, D., Iwata, T., Tokutomi, S. & Kandori, H. Unique temperature dependence in the adduct formation between FMN and cysteine S-H group in the LOV2 domain of *Adiantum* phytochrome3. *Chem. Phys. Lett.* **410**, 59–63 (2005).
 41. Iwata, T., Nozaki, D., Tokutomi, S., Kagawa, T., Wada, M. & Kandori, H. Light-induced structural changes in the LOV2 domain of *Adiantum* phytochrome3 studied by low-temperature FTIR and UV-visible spectroscopy. *Biochemistry* **42**, 8183–8191 (2003).
 42. Swartz, T. E., Wenzel, P. J., Corchnoy, S. B., Briggs, W. R. & Bogomolni, R. A. Vibration spectroscopy reveals light-induced chromophore and protein structural changes in the LOV2 domain of the plant blue-light receptor phototropin 1. *Biochemistry* **41**, 7183–7189 (2002).
 43. Corchnoy, S. B., Swartz, T. E., Lewis, J. W., Szundi, I., Briggs, W. R. & Bogomolni, R. A. Intramolecular proton transfers and structural changes during the photocycle of the LOV2 domain of phototropin 1. *J. Biol. Chem.* **278**, 724–731 (2003).
 44. Harper, S. M., Neil, L. C. & Gardner, K. H. Structural basis of a phototropin light switch. *Science* **301**, 1541–1544 (2003).
 45. Harper, S. M., Christie, J. M. & Gardner, K. H. Disruption of the LOV- α helix interaction activates phototropin kinase activity. *Biochemistry* **43**, 16184–16192 (2004).
 46. Eitoku, T., Nakasone, Y., Matsuoka, D., Tokutomi, S. & Terazima, M. Conformational dynamics of phototropin 2 LOV2

- domain with the linker upon photoexcitation. *J. Am. Chem. Soc.* **127**, 13238–13244 (2005).
47. Nakasone, Y., Eitoku, T., Matsuoka, D., Tokutomi, S. & Terazima, M. Kinetic measurement of transient dimerization and dissociation reactions of *Arabidopsis* phototropin 1 LOV2 domain. *Biophys. J.* **91**, 645–653 (2006).
 48. Nakasone, Y., Eitoku, T., Matsuoka, D., Tokutomi, S. & Terazima, M. Dynamics of conformational changes of *Arabidopsis* phototropin 1 LOV2 with the linker domain. *J. Mol. Biol.* **367**, 432–442 (2007).
 49. Eitoku, T., Nakasone, Y., Zikihara, K., Matsuoka, D., Tokutomi, S. & Terazima, M. Photochemical intermediates of *Arabidopsis* phototropin 2 LOV domains associated with conformational changes. *J. Mol. Biol.* **371**, 1290–1303 (2007).
 50. Nozaki, D., Iwata, T., Ishikawa, T., Todo, T., Tokutomi, S. & Kandori, H. Role of Gln1029 in the photoactivation processes of the LOV2 domain in *Adiantum* phytochrome3. *Biochemistry* **43**, 8373–8379 (2004).
 51. Iwata, T., Nozaki, D., Sato, Y., Sato, K., Nishina, Y., Shiga, K., Tokutomi, S. & Kandori, H. Identification of the C=O stretching vibrations of FMN and peptide backbone by ¹³C-labeling of the LOV2 domain of *Adiantum* phytochrome3. *Biochemistry* **45**, 15384–15391 (2006).
 52. Yamamoto, A., Iwata, T., Sato, Y., Matsuoka, D., Tokutomi, S., & Kandori, H. Light signal transduction pathway from flavin chromophore to J α helix of *Arabidopsis* phototropin1. *Biophys. J.* **96**, 2771–2778 (2009).
 53. Koyama, T., Iwata, T., Yamamoto, A., Sato, Y., Matsuoka, D., Tokutomi, S. & Kandori, H. Different role of the J α helix in the light-induced activation of the LOV2 domains in various phototropins. *Biochemistry* **48**, 7621–7628 (2009).
 54. Miura, R., Nishina, Y., Ohta, M., Tojo, H., Shiga, K., Watari, H., Yamano, T. & Miyake, Y. Resonance Raman study on the flavin in the purple intermediates of D-amino acid oxydase. *Biochem. Biophys. Res. Commun.* **111**, 588–594 (1983).
 55. Hazekawa, I., Nishina, Y., Sato, K., Shichiri, M., Miura, R. & Shiga, K. A Raman study on the C(4)=O stretching mode of flavins in flavoenzymes: Hydrogen bonding at the C(4)=O moiety. *J. Biochem.* **121**, 1147–1154 (1997).
 56. Nakasako, M., Iwata, T., Matsuoka, D. & Tokutomi, S. Light-induced structural changes of LOV domain-containing polypeptides from *Arabidopsis* phototropin 1 and 2 studied by small-angle X-ray scattering. *Biochemistry* **43**, 14881–14890 (2004).
 57. Matsuoka, D. & Tokutomi, S. Blue light-regulated molecular switch of Ser/Thr kinase in phototropin. *Proc. Natl. Acad. Sci. U.S.A.* **102**, 13337–13342 (2005).
 58. Nozaki, D., Iwata, T., Tokutomi, S. & Kandori, H. Water structural changes in the activation process of the LOV2 domain of *Adiantum* phytochrome3. *J. Mol. Struct.* **735/736**, 259–265 (2005).
 59. DeLano, W.L. The PyMOL molecular graphics system. DeLano Scientific, San Carlos, CA, USA. 2002.